Short communication

Fabrication of heterogeneous-based lacunary polyoxometalates as efficient catalysts for the multicomponent and clean synthesis of pyrazolopyranopyrimidines

Zahra Yekke-Ghasemi [a], Majid M. Heravi [a],[*], Masoume Malmir [a], Ghazaleh Jahani [a], Masoumeh Bagheri Bisafar [a], Masoud Mirzaei [b],[*]

[a] Department of Chemistry, School of Physics and Chemistry, Alzahra University, PO Box 1993891176, Vanak, Tehran, Iran
[b] Department of Chemistry, Faculty of Science, Ferdowsi University of Mashhad, Mashhad 9177948974, Iran

ABSTRACT

In continues efforts to the synthesis of polyoxometalate (POM) as catalysts, two lacunary POM-based heterogeneous catalysts $(TBA)_9[BW_{11}O_{39}] \cdot 11H_2O$ (**(TBA)$_9$BW$_{11}$**) and $(TBA)_6[Zr(OH)BW_{11}O_{39}] \cdot 8H_2O$ (**(TBA)$_6$BZrW$_{11}$**) (TBA^+: tetrabutylammonium) were synthesized and fully characterized using different techniques. The role of the cationic alkyl chains (TBA^+) not only leads to the formation of hydrophobic POM catalyst, but also reactants can be trapped near the POM center, which leads to higher catalytic efficiencies. Both catalysts can act as Lewis base due to their terminal oxygen atoms, while **(TBA)$_6$BZrW$_{11}$** have accessible Lewis acid sites (due to substituting zirconium site). Consequently, the catalytic utilities of these samples were investigated in the multicomponent synthesis of pyrazolopyranopyrimidine derivatives, which were attained in short times with high yields. These results established the efficiency of this protocol in terms of being environmentally friendly, high product yields, and being completed in short reaction times. Meanwhile, the synergetic effect between the catalysts components also played an essential role during the catalytic process.

1. Introduction

Multi-Component Reactions (MCRs), as a fascinating and hot topic of organic transformations, are effective, atom economical, and time-saving styles, which are often suitable alternatives to the consecutive multistep synthesis of small heterocyclic compounds and in the drug delivery and discovery processes [1-6]. Pyrazolopyranopyrimidine skeletons containing two active compounds, pyranopyrimidine, and pyranopyrazole, have been given particular attention due to their essential pharmacological and biological activities [7,8]. Pyrazolopyranopyrimidine can also be applied as a critical intermediate to the synthesis of biological and pharmaceutical compounds [9,10]. So far, many reports have been devoted to the synthesis of pyrazolopyranopyrimidines, some of which have disadvantages such as the use of large amounts of catalysts, toxic organic reagent and solvents, long process times and low yields [11-15]. Thus, the development of efficient approaches and exploitation of suitable and heterogeneous catalysts to rapidly build this compound is imperative.

Polyoxometalates (POMs) are discrete anionic metal–oxide clusters that can be formed by some transition metals in their highest oxidation state, including Mo(VI), W(VI), and V(V) (known as addenda atom) [16-18]. Due to the specific chemical and physical properties of POMs, they can be applied in the wide and diverse areas of research such as catalysts [19-21], sensors [22], magnetism [23], medicine [24], batteries [25] and so on. Up to now, POMs have been extensively used the catalysts as due to their interesting features such as: i) large negative charges which can act as Lewis bases in base-catalyzed reactions, ii) protons which can use as Brönsted acids in the promotion of acid-catalyzed reactions such as esterification, hydrolysis, and so on, iii) Lewis acidity of POMs that can be caused by the presence of metal ions with unoccupied orbitals such as substituted POMs with zirconium (IV), hafnium (IV), aluminum (III) or lanthanoid (III) ions [26]. In addition, the reversible multi-electron redox nature of POMs under the reaction conditions makes them proper catalysts for oxidation of alkanes, alcohols, olefins, and so on [27,28]. Notably, lacunary derivatives of POMs (LPOM) are known as species that have vacant site(s) on their structures and can be easily formed by the removal of some metal-oxide

Note: Low-resolution images were used to create this PDF. The original images will be used in the final composition.
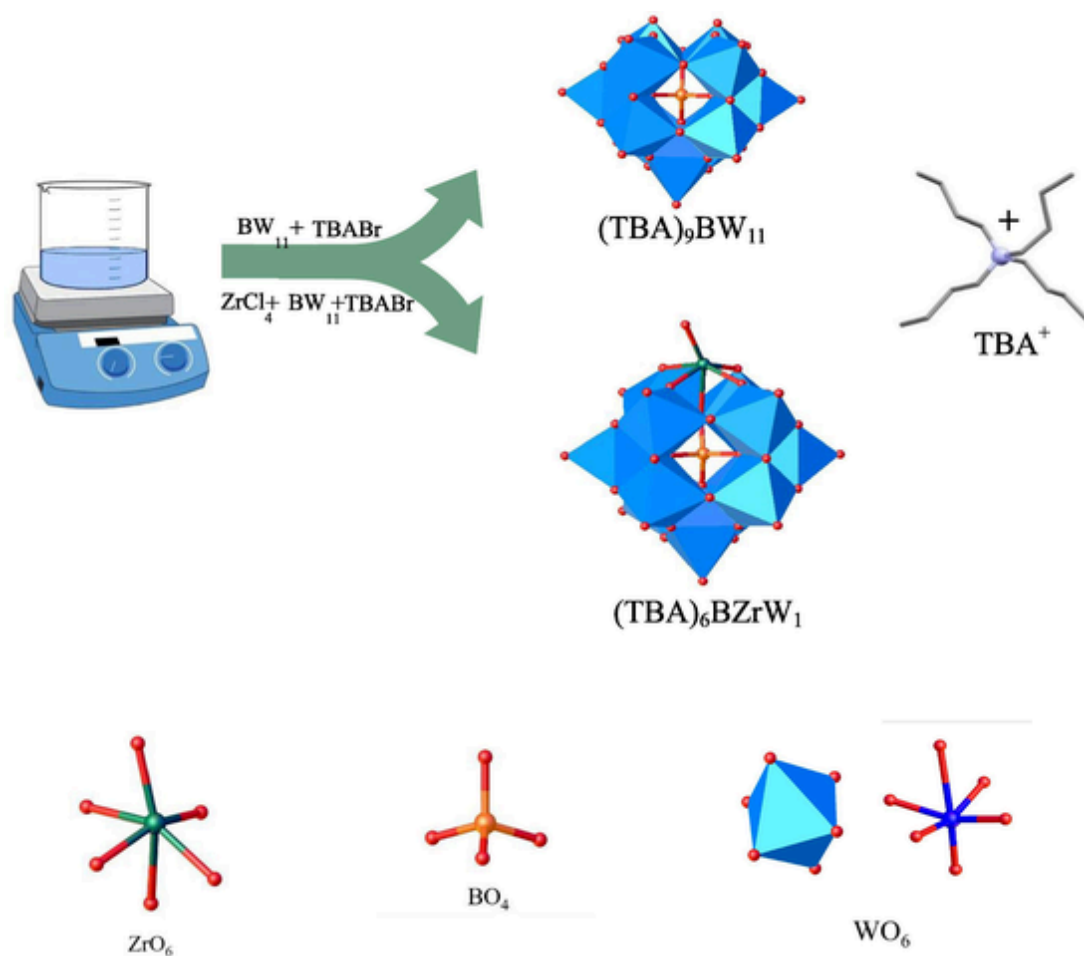
Fig. 1. Synthetic route of catalysts with representation of anionic structures of **(TBA)$_6$BZrW$_{11}$** and **(TBA)$_9$BW$_{11}$** heterogeneous catalysts, and cationic structure of TBA$^+$ (ball and mill and polyhedral representation).

[MO$_x$]$^{n+}$ unites and often will bind to a new addenda atom or certain metals and form substitute POMs with accessible Lewis acid sites. For example, Keggin-type POMs with total formula [XM$_{12}$O$_{40}$]$^{n-}$ (X = hetero atom, M = addenda atom) can form mono-, di- or tri-lacunary species [29]. The structure of mono-lacunary Keggins are more stable than other lacunary forms and have great protentional to bond with new metal ions [30] and also, depending on the metal inserted in certain application such as redox and acid/base properties can be tuned. For example, Lewis acidity of Zr^{IV} center in the Zr-containing POMs demonstrated a pronounced catalytic activity in many reactions such as oxidation reactions due to the available coordination sites on the Zr center [31-34].

Although POMs benefit from structural robustness, oxidative and thermal stability, the highly soluble nature of POMs (as homogeneous catalysts) makes them difficult for separation, so they cannot reuse again. Therefore, the heterogeneous approaches widely employed by researchers such as immobilization of POMs on solid supports with the high surface area like graphene, carbon nanotubes or metal–organic frameworks to create hybrid or composite materials [35-37] and encapsulation of POMs with specific cations [38]. In the latter case, POMs are usually covered by organic cations such as tetrabutylammonium (TBA$^+$) salts, dimethyldioctadecylammoum (DODA$^+$) salts, and so on to form heterogeneous systems which provide easier catalyst recovery, with simple filtration.

Following our attempt to investigate the synthesis and utility of novel lacunary POM-based catalysts for promoting organic transformations [39-42], and our interest in heterocyclic chemistry [43-50] and in novel pyrazolopyranopyrimidines [20,51-53] herein, we wish to pre-

sent two heterogeneous acidic catalytic systems based on the mono-lacunary borotungstate Keggin; (TBA)$_9$[BW$_{11}$O$_{39}$]·11H$_2$O (**(TBA)$_9$BW$_{11}$**) and (TBA)$_6$[Zr(OH)BW$_{11}$O$_{39}$]·8H$_2$O (**(TBA)$_6$BZrW$_{11}$**) as proficient catalysts to promote the synthesis of pyrazolopyranopyrimidine from the reaction of hydrazine hydrate/phenylhydrazine, malononitrile/barbituric acid, 1,3-dicarbonyl derivatives and aromatic aldehydes. As we expected, these catalysts would simultaneously be acted as Lewis acid/base, and by a combination of Zr^{4+} Lewis acid into the vacant binding site of lacunary Keggin, the catalytic activity of the resulted catalyst should be increased (Fig. 1). Moreover, to disclose the nature and stability of the catalyst, the recyclability of the **(TBA)$_6$BZrW$_{11}$** is also studied.

2. Methods

2.1. Chemicals and materials

The chemical compounds were purchased from Merck (Darmstadt, Germany) and Sigma-Aldrich (St. Louis, MO, USA) and used with no crystallization or purification. To conduct MCRs, aromatic aldehydes, hydrazine hydrate, phenylhydrazine, ethylacetoacetate, malononitrile, barbituric acid, toluene, ethanol, methanol, acetonitrile, and deionized water were used.

2.2. Instrumentation

Electrothermal 9200 apparatus was employed to determine the melting point of products. Bruker Tensor 27 FT-IR spectrometer
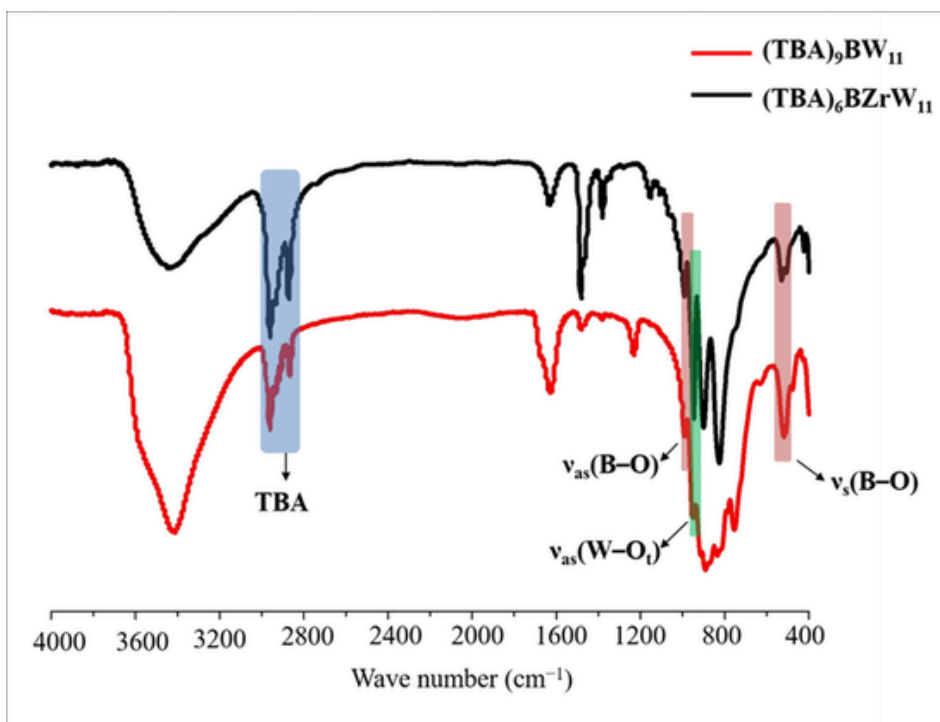
Fig. 2. FTIR spectra of **(TBA)$_9$BW$_{11}$** and **(TBA)$_6$BZrW$_{11}$** heterogeneous catalysts.

Table 1

Representation of important absorption bands (cm^{-1}) for **(TBA)$_9$BW$_{11}$** and **(TBA)$_6$BZrW$_{11}$** heterogeneous catalysts.

Compound	ν_{as}(B–O$_a$)	ν_s(B–O$_a$)	ν_{as}(W–O$_t$)	ν_{as}(W–O$_b$) and ν_{as}(W–O$_c$)
(TBA)$_9$BW$_{11}$	991	518	948	891, 837
(TBA)$_6$BZrW$_{11}$	991	530	947	899, 824

(400–4000 cm^{-1} region) was used to detect absorbance bands of KBr disk containing the compounds. Also, the infrared spectra of catalysts were recorded in the range of 4000–400 cm^{-1} on a Thermo Nicolet/AVATAR 370 Fourier transform spectrophotometer using the KBr discs. Elemental analysis (CHN) was performed using a Thermo Finnigan Flash EA 1112 microanalyzer. Metal content was measured by the Spectro Arcos ICP-OES spectrometer model 76004555 using in the range of 130–770 nm, and an ICP-AES analyzer (Varian, Vista-pro) was used for metal leaching of the sample in the course of recycling. The NMR measurements were recorded on a Bruker FUM-300 spectrometer using DMSO-d_6 as the solvent and residual solvent signal as an internal reference. The instruments used for performing FTIR spectroscopy by applying PERKIN/ELMER Spectrum 65 apparatus. Melting points were measured by Electrothermal 9100. To monitor of the MCR process, TLC on profitable aluminum-backed plates of silica gel 60 was applied and then visualized by UV–Vis light.

2.3. Preparation of catalysts

The mono-lacunary Keggin H$_2$K$_7$[BW$_{11}$O$_{39}$]·13H$_2$O (BW$_{11}$) was synthesized according to a literature method and identified by FT-IR and elemental analysis [54]. Then, heterogeneous catalysts were synthesized from BW$_{11}$.

2.3.1. Synthesis of (TBA)$_9$[BW$_{11}$O$_{39}$]·11H$_2$O

An aqueous solution of BW$_{11}$ (1 mmol, 10 ml) was added to the chloroform solution of TBABr (9 mmol, 10 ml). Then, the reaction mixture was stirred (2 h). After that, BW$_{11}$ was transferred into chloroform solution, so organic phase was separated and white precipitation of the product was collected by evaporation of the solvent and washed with deionized water two times. (Yield: 4.05 g, 30 % based on W). Anal. Calcd. for C$_{144}$H$_{346}$N$_9$BW$_{11}$O$_{50}$: C, 34.33; W, 40.14; N, 2.50; B, 0.21; H, 6.92 %. Found: C, 33.56; W, 39.75; N, 2.78; B, 0.29; H, 7.15 %. FT-IR (KBr pellet, cm^{-1}): 3411, 2961, 2929, 2876, 1627, 1484, 1384, 1231, 991, 948, 910, 891, 837, 754, 637, 518, 477. ^{1}H NMR (d_6-DMSO, 300 MHz, RT) [δ, ppm] 0.91–0.96 (t, TBA-CH$_3$), 1.27–1.39 (h, TBA-CH$_2$), 1.53–1.63 (dq, TBA-CH$_2$), 3.15–3.21 (m, TBA-CH$_2$). ^{13}C NMR (d_6-DMSO, 300 MHz, RT) [δ, ppm] 14.04, 19.70, 23.58, 57.99 (all singlets).

2.3.2. Synthesis of (TBA)$_6$[Zr(OH)BW$_{11}$O$_{39}$]·8H$_2$O

An aqueous solution of ZrCl$_4$ (0.73 mmol, 1 ml) added dropwise to the hot aqueous solution of BW$_{11}$ (0.67 mmol, 8 ml) and stirred (15 min). Then, a hot water solution of TBABr (6 mmol, 7 ml) added to the above mixture and stirred for further 30 min. The withe precipitation of the product collected by filtration and washed twice with water. (Yield: 5.5 g, 20 % based on W). Anal. Calcd. for C$_{96}$H$_{233}$N$_6$BZrW$_{11}$O$_{48}$: C, 26.42; W, 47.69; Zr, 2.09; N, 1.93; B, 0.25; H, 5.38 %. Found: C, 27.15; W, 48.21; Zr, 2.86; N, 2.47; B, 0.37; H, 5.91 % FT-IR (KBr pellet, cm^{-1}): 3445, 2960, 2933, 2872, 1631, 1438, 1381, 1152, 1111, 991, 947, 899, 824, 530, 506, 423. ^{1}H NMR (d_6-DMSO, 300 MHz, RT) [δ, ppm] 0.91–0.95 (t, TBA-CH$_3$), 1.27–1.40 (h, TBA-CH$_2$), 1.52–1.63 (m, TBA-CH$_2$), 3.15–3.21 (m, TBA-CH$_2$). ^{13}C NMR (d_6-DMSO, 300 MHz, RT) [δ, ppm] 13.99, 19.61, 23.54, 57.95 (all singlets).

2.4. Typical method for synthesis of pyrazolopyranopyrimidines

A mixture of aromatic aldehydes (1.0 mmol), hydrazine hydrate/phenylhydrazine (1.0 mmol), barbituric acid/malononitrile (1.0 mmol), ethyl acetoacetate (1.0 mmol), and catalyst (30 mg) in water (5 ml) was prepared and heated at 90 °C for the appropriate length of time. At the end of this reaction (checked by TLC), the reaction stopped and cooled to ambient temperature, and then the solid catalyst was filtrated, washed with H$_2$O/EtOH (1:1), and dried under air for reusing in consecutive reaction runs. Finally, for dissolving solid product, hot EtOH was added, and the white solution was recrystallized to obtain related product.

Table 2

Effects of catalyst's amount, temperature, and solvent on the yield of pyrazolopyranopyrimidine *via* model reaction.[a]
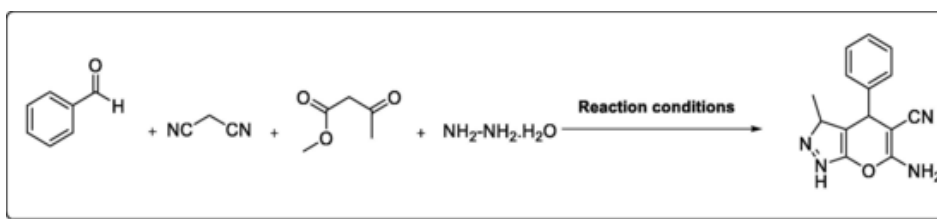
Entry	Catalyst (mg)	Condition Solvent/ Temperature (ºC)	Time (min)	Yield (%)[b]
1	None	H_2O/ 80	120	Trace
2	10	H_2O/ 80	30	50
3	20	H_2O/ 80	30	95
4	30	H_2O/ 80	30	95
5	20	H_2O/ r.t.	30	Trace
6	20	H_2O/ 50	30	50
7	20	H_2O/ 100	30	75
8	20	H_2O:EtOH (1:1)/ 80	30	80
9	20	EtOH/ Reflux	30	75
10	20	CH_3CN/ Reflux	30	35
11	20	Toluene/ Reflux	30	Trace
12	20	Solvent free/ 80	30	40

[a] Reaction condition: a mixture of hydrazine hydrate (1 mmol), ethyl acetoacetate (1 mmol), malononitrile (1 mmol), benzaldehyde (1 mmol), solvent (3 ml) and **(TBA)$_6$BZrW$_{11}$** as a catalyst was reacted.

[b] Isolated yield.

3. Result and discussion

### 3.1. Synthesis and characterization of catalysts

Two heterogeneous catalysts **(TBA)$_9$BW$_{11}$** and **(TBA)$_6$BZrW$_{11}$** of this study were obtained by reaction of mono-lacunary Keggin $[BW_{11}O_{39}]^{9-}$ under optimum conditions (Fig. 1). According to similar examples, POMs can be surrounded by alkyl chains (like TBA$^+$) [55, 56], and ^{1}H NMR and ^{13}C NMR spectra provide clear and direct evidence for the presence TBA$^+$ in the above catalysts. For example, in the ^{1}H NMR, three peaks located separately around 1.33, 1.57, and 3.18 ppm can be assigned to the CH$_2$ of TBA$^+$ and the CH$_3$ group located at 0.94 ppm (Figures S1-S4). Powder XRD of mono-lacunary Keggin appears at around 9-10° for 2θ value [57]. This characteristic peak is also present in powder XRD of **(TBA)$_9$BW$_{11}$** (8.9°) and **(TBA)$_6$BZrW$_{11}$** (8.6°) (Figure S5) with the minor shifts. Other characteristic peaks present in powder XRD of **(TBA)$_9$BW$_{11}$** were also present in the **(TBA)$_6$BZrW$_{11}$** along in the same plane with the minor shifts. These minor shifts may be due to the lattice strain produced by the attachment of zirconium to the BW$_{11}$ unit. It is important to note that POMs mainly act as Lewis base catalysts due to their terminal oxygen atoms, while substitute POMs with zirconium have accessible Lewis acid sites, which can improve the performance of the related catalyst [31,33,58].

Infrared spectroscopy is a frequently employed technique for the characterization of POMs due to their characteristic metal–oxygen stretching vibrations that occur in the region between 400 and 1000 cm^{-1}, which is known as the fingerprint region for the POMs (Fig. 2 and Table 1). The absorption bands at around 1630 and 3400 cm^{-1} attributed to the water molecules. Also, the characteristic strong bands for B-O, W–Ot, W–Ob, and W–Oc stretching vibrations of BW$_{11}$ are at around 991, 948, 891(899), and 824(837) cm^{-1}, respectively. Moreover, absorptions in the range 2872–2960 cm^{-1} correspond to the C–H stretching vibrations of TBA.

3.2. Catalytic activity

In the following and to elucidate the catalytic activity of **(TBA)$_9$BW$_{11}$** and **(TBA)$_6$BZrW$_{11}$**, the four-component one-pot synthesis of pyrazolopyranopyrimidines was investigated. In this context, the reaction of ethyl acetoacetate, benzaldehyde, NH$_2$-NH$_2$·H$_2$O, and malononitrile was elected as a model reaction, and the catalytic performance of two catalysts were investigated and compared (Table 2). The results demonstrated that both samples exhibited excellent catalytic activity but **(TBA)$_6$BZrW$_{11}$** was much better in isolation. In detail, **(TBA)$_6$BZrW$_{11}$** is insoluble in hot water and can be separated by simple filtration, while **(TBA)$_9$BW$_{11}$** is partly soluble and has a difficult separation from the reaction mixture. For this purpose, **(TBA)$_6$BZrW$_{11}$** was selected to continue catalytic research, and subsequently, the reaction parameters, including catalyst's loading, temperature, and solvent were optimized. Hence, the model reaction was performed without any catalyst and additive (Table 2, entry 1). It was found that this reaction profits very slowly (2 h) and a low amount of the product was achieved. Hence, the low amount of **(TBA)$_6$BZrW$_{11}$** was studied on a model reaction, and desired product was achieved in 50% yield (Table 2, entry 2). While, the higher amount of **(TBA)$_6$BZrW$_{11}$** did not significantly affect the reaction (Table 2, entry 4), which could be due to the rapid interaction of the reagents with each other in the presence of a large amount of catalyst, which subsequently led to the formation of a by-product and incomplete reaction. Moreover, the optimum catalyst amount was found to be 20 mg (Table 2, entry 3). Next, the solvent was optimized by using several solvents, and water was selected as a green and suitable reaction solvent (Table 2, entries 8–12). Generally, a comparison of the yield of the corresponding product in water as a solvent was superior to aprotic and non-protic solvents such as toluene or acetonitrile, which could be due to the homogenization of the reaction medium and the creation of a suitable substrate for effective interaction between the reactants. As can be seen from the results of Table 2, polar solvents, especially water, accelerate the reaction due to the close bonds and effective interactions between the reactants, while non-polar solvents such as toluene and acetonitrile do not allow this. Finally, the efficacy of

Table 3

Synthesis of pyrazolopyranopyrimidine derivatives via a four-component reaction catalyzed by (TBA)6BZrW11.[a]
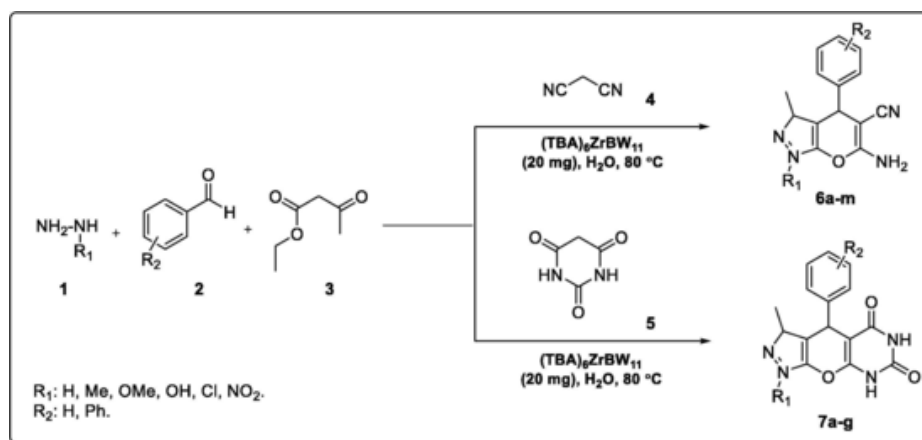
Entry	R_1	R_2	Product	Time (h:min)	Yields[b] (%)
1	H	H	6a	(0:30)	(95)
2	H	4-Cl	6b	(1:15)	(95)
3	H	4-NO$_2$	6c	(0:45)	(85)
4	H	4-MeO	6d	(0:50)	(80)
5	H	2-MeO	6e	(0:55)	(75)
6	H	4-C$_3$H$_5$	6f	(1:30)	(50)
7	H	2-OH	6g	(1:40)	(75)
8	Ph	4-Cl	6h	(2:30)	(70)
9	Ph	4-NO$_2$	6i	(0:55)	(80)
10	Ph	4-MeO	6j	(1:05)	(75)
11	Ph	2-MeO	6k	(1:20)	(65)
12	Ph	4-C$_3$H$_5$	6l	(2:00)	(55)
13	Ph	2-OH	6m	(3:00)	(60)
14	H	H	7a	(1:15)	(85)
15	H	4-MeO	7b	(2:30)	(70)
16	H	4-Me	7c	(5:00)	(30)
17	H	4-NO$_2$	7d	(2:00)	(80)
18	Ph	4-MeO	7e	(3:30)	(40)
19	Ph	4-Me	7f	(4:00)	(55)
20	Ph	4-NO$_2$	7g	(2:30)	(75)

[a] Reaction conditions: Hydrazine hydrate or phenyl hydrazine (1 mmol), ethyl acetoacetate (1 mmol), malononitrile (1 mmol), aromatic aldehyde (1 mmol), **(TBA)$_6$BZrW$_{11}$** (20 mg) and H$_2$O (3 ml) at 80 ˚C.

[b] Isolated yield.

temperature on the product's yield was studied. The productivity of the catalysts on this reaction is noticeably dependent on the temperature. When it was set to room temperature, related product was attained in low yield (Table 2, Entry 5). Noteworthy, increasing temperature to 50 ˚C, the product's yield dramatically enhanced (Table 2, Entry 6). However, a further increase to 80 ˚C had a positive effect, and the higher temperature was not suitable at all (Table 2, entries 3 and 7). The results established that using 20 mg of the **(TBA)$_6$BZrW$_{11}$** in water as s solvent at 80 ˚C are ideal reaction parameters.

To test the generality of this protocol, various aromatic aldehydes, NH$_2$-NH$_2$·H$_2$O or phenylhydrazine, malononitrile or barbituric acid, and ethyl acetoacetate were examined under the optimized reaction conditions (Table 3). The outcomes established that aromatic aldehydes led to the formation of conforming products in moderate to excellent yields. However, aromatic aldehydes with electron with drawing groups resulted in higher yields in shorter reaction times. Comparison of 2 and 4 positions in substituted-aldehydes shows that, not only the nature of the substituent influences the yield, but so does its position. Yields increased in this order: 2 < 4. The largest effect is found for the methyl group at para position. Notably, the use of phenylhydrazine in-

stead of NH$_2$-NH$_2$·H$_2$O led to the formation of products **6h-6m** in longer reaction time with moderate yields. Furthermore, compared to barbituric acid, using malononitrile resulted in shorter times with higher yields. Based on these results, the effect of the electron density of the substrate on this reaction was confirmed. All organic products were known, and for identification, and their physical properties and spectral data were considered. Hence, some selected products were recognized by FTIR spectroscopy (see Supplementary material, Figure S6-S12).

It is clear, these experimental results are in good agreement with the reported reaction mechanism in Fig. 3. Initially, 3-methyl-1*H*-pyrazol-5 (4H)-one (I) was produced through the reaction of NH$_2$-NH$_2$ and ethyl acetoacetate promoted by LPMO. Following, the Knoevenagle condensation of barbituric acid and benzaldehyde leads to giving the intermediate (II). Then, intermediate (II) undergoes a Michael addition with intermediate (I) and generates a fresh intermediate (III) that endured ring closure and dehydration process to afford the triheterocyclic product (IV) and complete the catalytic cycle [20,59].

Next, to show the merits of the present protocol using the heterogeneous and inexpensive catalysts for the synthesis of pyrazolopyranopyrimidines, its catalytic activity on the model reaction was compared
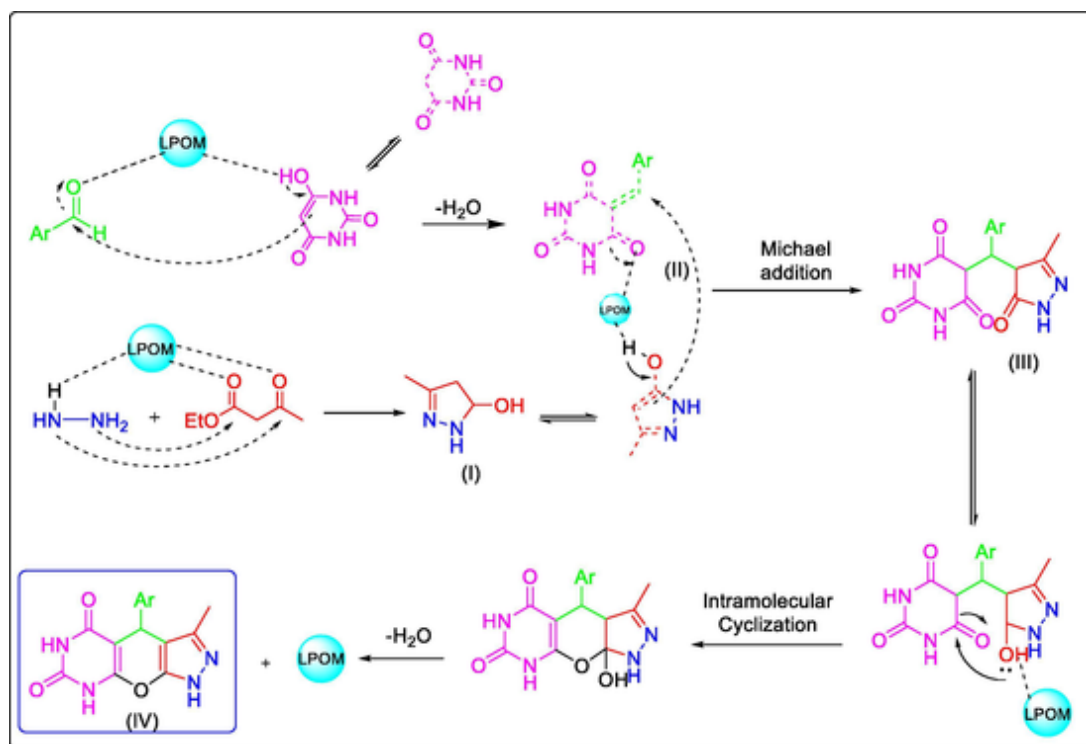
Fig. 3. The proposed mechanism of synthesis of pyrazolopyranopyrimidine.

Table 4

Comparison of the result using our reaction system with results obtained by other published works for the synthesis of pyrano[2,3-c]pyrazoles.

Entry	Catalysts (amount)	Reaction conditions Solvent/ Temperature (°C)	Time (min)	Yields[b] (%)	Ref
1	Fe$_3$O$_4$@SiO$_2$@PTS-DABA (10 mg)	EtOH/ 70	(23)	(88)	[60]
2	MIL-53(Fe) (5 mg)	EtOH/ r.t.	(20)	(91)	[61]
3	Borax (40 mg)	H$_2$O/ Reflux	(50)	(85)	[62]
4	ACS-SO$_3$H (5 mg)	[CholineCl][Urea]$_2$/ r.t.	(67)	(52)	[62]
5	Sodium Citrate (5 mol%)	EtOH/ Reflux	(60)	(80)	[63]
6	**(TBA)$_9$BW$_{11}$**	H$_2$O/ 80	(30)	(75)	This work
7	**(TBA)$_6$BZrW$_{11}$**	H$_2$O/ 80	(30)	(95)	This work

[a]Reaction condition: a mixture of hydrazine hydrate (1 mmol), ethyl acetoacetate (1 mmol), malononitrile (1 mmol), benzaldehyde (1 mmol), solvent (3 ml) and catalyst were reacted.

[b] Isolated yield.

with some of the earlier reported methodologies, Table 4. As tabulated, this reaction was performed under different reaction conditions. According to Table 4, low catalyst amount, reusability of **(TBA)$_6$BZrW$_{11}$**, and short reaction time are advantageous of the present protocol. Notably, in the case of using a homogeneous catalyst, the recyclability is comparative.

3.3. Characterization data

6-amino-3-methyl-4-phenyl-2,4-dihydropyrano[2,3-c] pyrazole-5-carbonitrile (6a) [64]. Yield: (95 %); White solid; M.p. 241–243 °C; FTIR (KBr): 3372, 3309, 3167, 2191, 1648, 1595, 1487, 1427, 1071, 552 cm^{-1}.

6-amino-4-(4-chlorophenyl)-3-methyl-2,4-dihydropyrano[2,3-c] pyrazole-5-carbonitrile (6b) [64]. Yield: (95 %); White solid; M.p. 234–236 °C; FTIR (KBr): 3444, 3047, 2939, 2213, 1623, 1591, 1486, 1399, 1087, 680, 497 cm^{-1}.

6-amino-4-(4-nitrophenyl)-3-methyl-2,4-dihydropyrano [2,3-c] pyrazole-5-carbonitrile (6c) [64]. Yield: (85 %); Yellow solid; M.p. 249–251 °C; FTIR (KBr): 3379, 3252, 2984, 2217, 1636, 1517, 1346, 1283, 1183, 855 cm^{-1}.

6-amino-4-(4-methoxyphenyl)-3-methyl-2,4-dihydropyrano [2,3-c] pyrazole-5-carbonitrile (6d) [64]. Yield: (80 %); Cream solid; m.p. 209–211 °C; FTIR (KBr): 3386, 2927, 2843, 2210, 1603, 1510, 1461, 1302, 1252, 1168, 1026, 833 cm^{-1}.

6-amino-4-(4-chlorophenyl)-3-methyl-1-phenyl-1,4-dihydropyrano [2,3-c] pyrazole-5-carbonitrile (6h) [64]. Yield: (70 %); Cream solid; m.p. 170–172 °C; FTIR (KBr): 3445, 2923, 2251, 1649, 1600, 1502, 1404, 1292, 1017, 809, 746 cm^{-1}.

6-amino-4-(4-methoxyphenyl)-3-methyl-1-phenyl-1,4-dihydropyrano [2,3-c] pyrazole-5-carbonitrile (6j) [64]. Yield: (75 %); White solid; m.p. 170–172 °C; IR (KBr): 3397, 3312, 2926, 2222, 1604, 1569, 1511, 1370, 1277, 1183, 1023, 833 cm^{-1}.

3-Methyl-4-(4-methylphenyl)-1,4-dihydropyrazolo [4′,3′:5,6] pyrano [2,3-d] pyrimidine-5,7(6H,8H)-dione (7b) [20]. Yield: (70 %); White solid; m.p. 200–202 °C; IR (KBr): 3213, 3026, 2925, 1695, 1597, 1512, 1458, 1367, 1024, 810 cm^{-1}.

3.4. Reusability of the catalyst

Along with the excellence catalytic activity of heterogeneous catalysts, simple recovery and facile reusability are important requisites for in sake of manufacturing use. Henceforth, the study on the ability of the catalysts to reuse is imperative. To empirically investigate the reusability of **(TBA)$_9$BW$_{11}$** and **(TBA)$_6$BZrW$_{11}$**, the model reaction was performed in their presence under optimal conditions. After finishing the multicomponent reactions, **(TBA)$_6$BZrW$_{11}$** was basically filtered, washed, dried, and then applied for the next reaction runs. As displayed in Figure S13, **(TBA)$_6$BZrW$_{11}$** could be separated and successfully recycled for three reaction cycles with loss of catalytic activity. However, the **(TBA)$_9$BW$_{11}$** catalyst was difficult to isolate from the reaction mix-
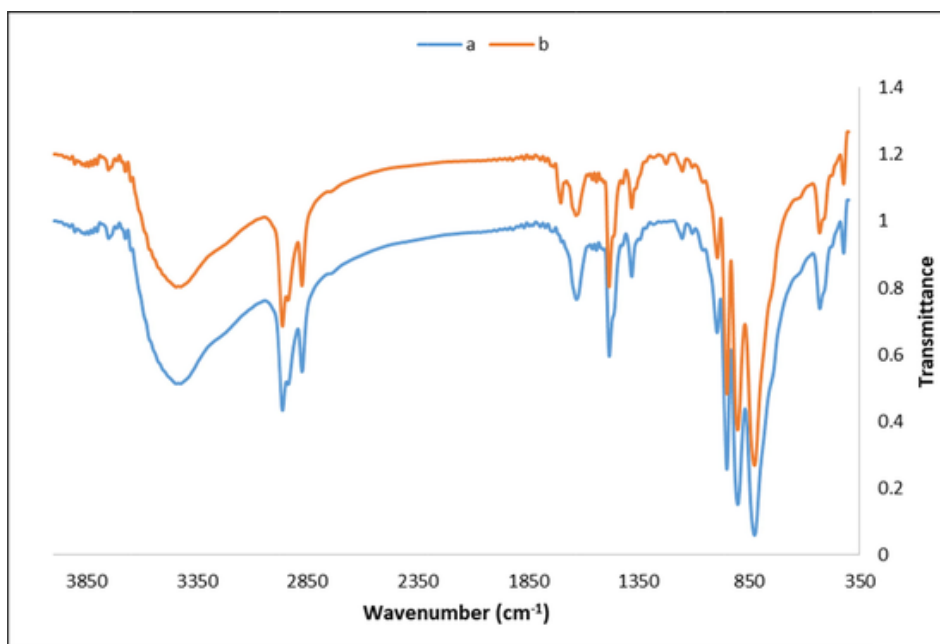
Fig. 4. The comparison of FTIR analyses for fresh $(TBA)_6BZrW_{11}$ (a) and after three runs (b).

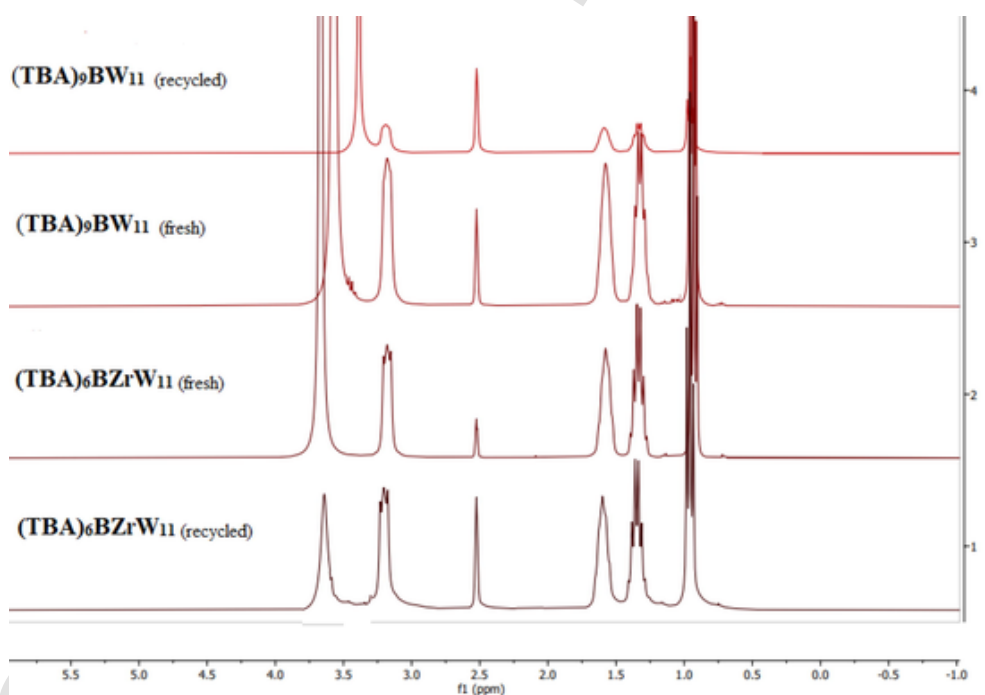**Fig. 5.** The ^1H NMR analyses of fresh and recycled $(TBA)_9BW_{11}$ and $(TBA)_6BZrW_{11}$.

ture, and it was not possible to study the recovery conditions. Preserving the catalytic performance of $(TBA)_6BZrW_{11}$ and slight loss of productivity after the final reaction run, it can be inferred that the leaching of lacunary POM is insignificant in solution.

To elucidate this reason, the FTIR spectrum of reused $(TBA)_6BZrW_{11}$ was attained, and it was compared with that of the fresh catalyst and demonstrated in Fig. 4. Remarkably, these results established that both FTIR spectra were almost similar with some extra bands in reused catalyst, indicating that the catalyst's structure was almost preserved in the progress of the reaction. This consequence can be mainly attributed to the deposition of various organic species on the surface of $(TBA)_6BZrW_{11}$ in the course of several reactions runs.

Moreover, ^1H NMR analysis of fresh and recycled catalysts was performed, to check the structural integrity of $(TBA)_9BW_{11}$ and $(TBA)_6BZrW_{11}$, and no momentous changes in their patterns were detected (Fig. 5).

4. Conclusion

In the present study, two heterogeneous catalysts based on polyoxometalates $(TBA)_9BW_{11}$ and $(TBA)_6BZrW_{11}$ were synthesized and characterized using a suite of analytical techniques. Notably, alkylammonium cations (TBA^+) on the surface of POMs provide flexible structures with hydrophobic and polar nature that promote catalytic performance by trapping organic reactants on the catalyst surface. $(TBA)_6BZrW_{11}$ in-

dicated to be a heterogeneous and useful catalyst for the preparation of pyrazolopyranopyrimidines *via* two pathways to give the expected products in significant yields compared to many other heterogeneous catalysts. Also, further studies are underway in our laboratory to extend the application of these family catalysts to other coupling reactions.

CRediT authorship contribution statement

Zahra Yekke-Ghasemi: Methodology, Formal analysis, Investigation, Software, Data curation, Writing – original draft. **Majid M. Heravi:** Conceptualization, Funding acquisition, Supervision, Writing – review & editing, Project administration, Visualization. **Masoume Malmir:** Methodology, Formal analysis, Investigation, Software, Data curation, Writing – original draft. **Masoud Mirzaei:** Methodology, Conceptualization, Funding acquisition, Supervision, Writing – review & editing, Project administration, Visualization.

Declaration of Competing Interest

The authors declare that they have no known competing financial interests or personal relationships that could have appeared to influence the work reported in this paper.

Acknowledgement

Appendix A. Supplementary material

Supplementary data to this article can be found online at https://doi.org/10.1016/j.inoche.2022.109456.

References

[1] I. Nakamura, Y. Yamamoto, Transition-metal-catalyzed reactions in heterocyclic synthesis, Chem. Rev. 104 (2004) 2127–2198, https://doi.org/10.1021/cr020095i.

[2] S.E. John, S. Gulati, N. Shankaraiah, Recent advances in multi-component reactions and their mechanistic insights: a triennium review, Org. Chem. Front. 8 (2021) 4237–4287, https://doi.org/10.1039/D0QO01480J.

[3] X. Zhu, C. Ran, M. Wen, G. Guo, Y. Liu, L. Liao, Y. Li, M. Li, D. Yu, Prediction of multicomponent reaction yields using machine learning, Chinese J. Chem. 39 (2021) 3231–3237, https://doi.org/10.1002/cjoc.202100434.

[4] S.-C. Zhan, R.-J. Fang, J. Sun, C.-G. Yan, Multicomponent reaction for diastereoselective synthesis of spiro[carbazole-3,4′-pyrazoles] and spiro[carbazole-3,4′-thiazoles], J. Org. Chem. 86 (2021) 8726–8741, https://doi.org/10.1021/acs.joc.1c00538.

[5] S. Maddila, S.B. Jonnalagadda, K.K. Gangu, S.N. Maddila, Recent advances in the synthesis of pyrazole derivatives using multicomponent reactions, Curr. Org. Synth. 14 (2017), https://doi.org/10.2174/1570179414666161208164731.

[6] A One-Pot Multicomponent Catalytic Synthesis of New 1H-Pyrazole-1-Carbothioamide Derivatives with Molecular Docking Studies as COX-2 Inhibitors, Biointerface Res. Appl. Chem. 11 (2021) 13779–13789. Doi: 10.33263/BRIAC116.1377913789.

[7] H.N. Hafez, A.G. Alshammari, A.-R.-B.-A. El-Gazzar, Facile heterocyclic synthesis and antimicrobial activity of polysubstituted and condensed pyrazolopyranopyrimidine and pyrazolopyranotriazine derivatives, Acta Pharm. 65 (2015) 399–412, https://doi.org/10.1515/acph-2015-0037.

[8] M. Bakherad, A. Keivanloo, M. Gholizadeh, R. Doosti, M. Javanmardi, Using magnetized water as a solvent for a green, catalyst-free, and efficient protocol for the synthesis of pyrano[2,3-c]pyrazoles and pyrano[4′,3′:5,6]pyrazolo [2,3-d] pyrimidines, Res. Chem. Intermed. 43 (2017) 1013–1029, https://doi.org/10.1007/s11164-016-2680-y.

[9] A.R. Bhat, A.H. Shalla, R.S. Dongre, Microwave assisted one-pot catalyst free green synthesis of new methyl-7-amino-4-oxo-5-phenyl-2-thioxo-2,3,4,5-tetrahydro-1H-pyrano[2,3-d]pyrimidine-6-carboxylates as potent in vitro antibacterial and antifungal activity, J. Adv. Res. 6 (2015) 941–948, https://doi.org/10.1016/j.jare.2014.10.007.

[10] B.P. Bandgar, S.S. Gawande, R.G. Bodade, N.M. Gawande, C.N. Khobragade, Synthesis and biological evaluation of a novel series of pyrazole chalcones as anti-inflammatory, antioxidant and antimicrobial agents, Bioorg. Med. Chem. 17 (2009) 8168–8173, https://doi.org/10.1016/j.bmc.2009.10.035.

[11] X.-T. Li, A.-D. Zhao, L.-P. Mo, Z.-H. Zhang, Meglumine catalyzed expeditious

[12] four-component domino protocol for synthesis of pyrazolopyranopyrimidines in aqueous medium, RSC Adv. 4 (2014) 51580–51588, https://doi.org/10.1039/C4RA08689A.

[12] M.R. Tipale, L.D. Khillare, A.R. Deshmukh, M.R. Bhosle, An efficient four component domino synthesis of pyrazolopyranopyrimidines using recyclable choline chloride: urea deep eutectic solvent, J. Heterocycl. Chem. 55 (2018) 716–728, https://doi.org/10.1002/jhet.3095.

[13] F. Rigi, H.R. Shaterian, Magnetic nanoparticle supported ionic liquid assisted green synthesis of pyrazolopyranopyrimidines and 1,6-diamino-2-oxo-1,2,3,4-tetrahydropyridine-3,5- dicarbonitriles, J. Chinese Chem. Soc. 63 (2016) 557–561, https://doi.org/10.1002/jccs.201500407.

[14] K.K. Gangu, S. Maddila, S.N. Maddila, S.B. Jonnalagadda, Novel iron doped calcium oxalates as promising heterogeneous catalysts for one-pot multicomponent synthesis of pyranopyrazoles, RSC Adv. 7 (2017) 423–432, https://doi.org/10.1039/C6RA25372E.

[15] S. Ambethkar, V. Padmini, N. Bhuvanesh, A green and efficient protocol for the synthesis of dihydropyrano[2,3-c]pyrazole derivatives via a one-pot, four component reaction by grinding method, J. Adv. Res. 6 (2015) 975–985, https://doi.org/10.1016/j.jare.2014.11.011.

[16] P. Yang, U. Kortz, Discovery and evolution of polyoxopalladates, Acc. Chem. Res. 51 (2018) 1599–1608, https://doi.org/10.1021/acs.accounts.8b00082.

[17] M. Mirzaei, H. Eshtiagh-Hosseini, M. Alipour, A. Frontera, Recent developments in the crystal engineering of diverse coordination modes (0–12) for Keggin-type polyoxometalates in hybrid inorganic–organic architectures, Coord. Chem. Rev. 275 (2014) 1–18, https://doi.org/10.1016/j.ccr.2014.03.012.

[18] S. Taleghani, M. Mirzaei, H. Eshtiagh-Hosseini, A. Frontera, Tuning the topology of hybrid inorganic–organic materials based on the study of flexible ligands and negative charge of polyoxometalates: A crystal engineering perspective, Coord. Chem. Rev. 309 (2016) 84–106, https://doi.org/10.1016/j.ccr.2015.10.004.

[19] N. Narkhede, S. Singh, A. Patel, Recent progress on supported polyoxometalates for biodiesel synthesis via esterification and transesterification, Green Chem. 17 (2015) 89–107, https://doi.org/10.1039/C4GC01743A.

[20] N. Lotfian, M.M. Heravi, M. Mirzaei, M. Daraie, Investigation of the uncommon basic properties of [Ln(W5O18)2]9– (Ln = La, Ce, Nd, Gd, Tb) by changing central lanthanoids in the syntheses of pyrazolopyranopyrimidines, J. Mol. Struct. 1199 (2020) 126953, https://doi.org/10.1016/j.molstruc.2019.126953.

[21] M.M. Heravi, M. Mirzaei, S.Y.S. Beheshtiha, V. Zadsirjan, F. Mashayekh Ameli, M. Bazargan, $H_5 BW_{12} O_{40}$ as a green and efficient homogeneous but recyclable catalyst in the synthesis of *4* H -Pyran*s via* multicomponent reaction, Appl. Organomet. Chem. 32 (2018) e4479, https://doi.org/10.1002/aoc.4479.

[22] C. Zhou, S. Li, W. Zhu, H. Pang, H. Ma, A sensor of a polyoxometalate and Au-Pd alloy for simultaneously detection of dopamine and ascorbic acid, Electrochim. Acta. 113 (2013) 454–463, https://doi.org/10.1016/j.electacta.2013.09.109.

[23] Z. Koshkhan, M. Mirzaei, H. Eshtiagh-Hosseini, M. Izadyar, J.T. Mague, M. Korabik, Two polyoxometalate-based hybrids constructed from trinuclear lanthanoid clusters with single-molecule magnet behavior, Polyhedron. 194 (2021) 114903, https://doi.org/10.1016/j.poly.2020.114903.

[24] M. Arefian, M. Mirzaei, H. Eshtiagh-Hosseini, A. Frontera, A survey of the different roles of polyoxometalates in their interaction with amino acids, peptides and proteins, Dalton Trans. 46 (2017) 6812–6829, https://doi.org/10.1039/C7DT00894E.

[25] H. Wang, S. Hamanaka, Y. Nishimoto, S. Irle, T. Yokoyama, H. Yoshikawa, K. Awaga, In operando X-ray absorption fine structure studies of polyoxometalate molecular cluster batteries: polyoxometalates as electron sponges, J. Am. Chem. Soc. 134 (2012) 4918–4924, https://doi.org/10.1021/ja2117206.

[26] S. Herrmann, C. Ritchie, C. Streb, Polyoxometalate – conductive polymer composites for energy conversion, energy storage and nanostructured sensors, Dalton Trans. 44 (2015) 7092–7104, https://doi.org/10.1039/C4DT03763D.

[27] Z. Zhang, S. Ishikawa, Q. Zhu, T. Murayama, M. Sadakane, M. Hara, W. Ueda, Redox-active zeolitic transition metal oxides based on ε-Keggin units for selective oxidation, Inorg. Chem. 58 (2019) 6283–6293, https://doi.org/10.1021/acs.inorgchem.9b00502.

[28] R. Neumann, Activation of molecular oxygen, polyoxometalates, and liquid-phase catalytic oxidation, Inorg. Chem. 49 (2010) 3594–3601, https://doi.org/10.1021/ic9015383.

[29] Q. Jia, J. Cao, Y. Duan, C. Hu, The solution chemistry and reactivity of lacunary Keggin silicotungstates monitored in real-time by a combination of mass spectrometry and electrochemistry, Dalton Trans. 44 (2015) 553–559, https://doi.org/10.1039/C4DT02723J.

[30] M. Arab Fashapoyeh, M. Mirzaei, H. Eshtiagh-Hosseini, A. Rajagopal, M. Lechner, R. Liu, C. Streb, Photochemical and electrochemical hydrogen evolution reactivity of lanthanide-functionalized polyoxotungstates, Chem. Comm. 54 (2018) 10427–10430, https://doi.org/10.1039/C8CC06334F.

[31] N.V. Maksimchuk, V.Y. Evtushok, O.V. Zalomaeva, G.M. Maksimov, I.D. Ivanchikova, Y.A. Chesalov, I.V. Eltsov, P.A. Abramov, T.S. Glazneva, V.V. Yanshole, O.A. Kholdeeva, R.J. Errington, A. Solé-Daura, J.M. Poblet, J.J. Carbó, Activation of H_2O_2 over Zr(IV), insights from model studies on Zr-monosubstituted lindqvist tungstates, ACS Catal. 11 (2021) 10589–10603, https://doi.org/10.1021/acscatal.1c02485.

[32] O.A. Kholdeeva, G.M. Maksimov, R.I. Maksimovskaya, M.P. Vanina, T.A. Trubitsina, D.Y. Naumov, B.A. Kolesov, N.S. Antonova, J.J. Carbó, J.M. Poblet, Zr IV -monosubstituted Keggin-type dimeric polyoxometalates: synthesis, characterization, catalysis of H_2O_2 -based oxidations, and theoretical study, Inorg. Chem. 45 (2006) 7224–7234, https://doi.org/10.1021/ic0608142.

[33] H. Aoto, K. Matsui, Y. Sakai, T. Kuchizi, H. Sekiya, H. Osada, T. Yoshida, S. Matsunaga, K. Nomiya, Zirconium(IV)- and hafnium(IV)-containing

polyoxometalates as oxidation precatalysts: Homogeneous catalytic epoxidation of cyclooctene by hydrogen peroxide, J. Mol. Catal. A Chem. 394 (2014) 224–231, https://doi.org/10.1016/j.molcata.2014.07.020.

[34] D. Li, H. Han, Y. Wang, X. Wang, Y. Li, E. Wang, Modification of tetranuclear zirconium-substituted polyoxometalates – syntheses, structures, and peroxidase-like catalytic activities, Eur. J. Inorg. Chem. 2013 (2013) 1926–1934, https://doi.org/10.1002/ejic.201200791.

[35] S. Derakhshanrad, M. Mirzaei, C. Streb, A. Amiri, C. Ritchie, Polyoxometalate-based frameworks as adsorbents for drug of abuse extraction from hair samples, Inorg. Chem. 60 (2021) 1472–1479, https://doi.org/10.1021/acs.inorgchem.0c02769.

[36] M. Akbari, M. Mirzaei, A. Amiri, Synergistic effect of lacunary polyoxotungstates and carbon nanotubes for extraction of organophosphorus pesticides, Microchem. J. 170 (2021) 106665, https://doi.org/10.1016/j.microc.2021.106665.

[37] A. Amiri, M. Mirzaei, S. Derakhshanrad, A nanohybrid composed of polyoxotungstate and graphene oxide for dispersive micro solid-phase extraction of non-steroidal anti-inflammatory drugs prior to their quantitation by HPLC, Microchim. Acta. 186 (2019) 534, https://doi.org/10.1007/s00604-019-3694-0.

[38] A. Nisar, Y. Lu, J. Zhuang, X. Wang, Polyoxometalate nanocone nanoreactors: magnetic manipulation and enhanced catalytic performance, Angew. Chem. Int. Ed. 50 (2011) 3187–3192, https://doi.org/10.1002/anie.201006155.

[39] S. Sadjadi, M. Akbari, B. Léger, E. Monflier, M.M. Heravi, Eggplant-derived biochar-halloysite nanocomposite as supports of Pd nanoparticles for the catalytic hydrogenation of nitroarenes in the presence of cyclodextrin, ACS Sustain. Chem. Eng. 7 (2019) 6720–6731, https://doi.org/10.1021/acssuschemeng.8b05992.

[40] S. Sadjadi, G. Lazzara, M. Malmir, M.M. Heravi, Pd nanoparticles immobilized on the poly-dopamine decorated halloysite nanotubes hybridized with N-doped porous carbon monolayer: A versatile catalyst for promoting Pd catalyzed reactions, J. Catal. 366 (2018) 245–257, https://doi.org/10.1016/j.jcat.2018.08.013.

[41] S. Sadjadi, M. Malmir, G. Lazzara, G. Cavallaro, M.M. Heravi, Preparation of palladated porous nitrogen-doped carbon using halloysite as porogen: disclosing its utility as a hydrogenation catalyst, Sci. Rep. 10 (2020) 2039, https://doi.org/10.1038/s41598-020-59003-5.

[42] M. Heravi, M. Daraie, A novel and efficient five-component synthesis of pyrazole based pyrido[2,3-d]pyrimidine-diones in water: a triply green synthesis, Molecules. 21 (2016) 441, https://doi.org/10.3390/molecules21040441.

[43] M.M. Heravi, L. Mohammadkhani, Synthesis of various N-heterocycles using the four-component Ugi reaction, in: 2020, pp. 351–403. Doi: 10.1016/bs.aihch.2019.04.001.

[44] M.M. Heravi, B. Talaei, Diketene as Privileged Synthon in the Syntheses of Heterocycles Part 1, in: 2017, pp. 43–114. Doi: 10.1016/bs.aihch.2016.10.003.

[45] M.M. Heravi, B. Talaei, Ketenes as Privileged Synthons in the Synthesis of Heterocyclic Compounds Part 3, in: 2016, pp. 195–291. Doi: 10.1016/bs.aihch.2015.10.007.

[46] M.M. Heravi, V. Fathi Vavsari, Recent advances in application of amino acids: key building blocks in design and syntheses of heterocyclic compounds, in: 2015, pp. 77–145. Doi: 10.1016/bs.aihch.2015.02.002.

[47] M.M. Heravi, B. Talaei, Ketenes as Privileged Synthons in the Syntheses of Heterocyclic Compounds Part 2: Five-Membered Heterocycles, in: 2015, pp. 147–225. Doi: 10.1016/bs.aihch.2015.02.001.

[48] M.M. Heravi, V. Zadsirjan, Recent Advances in the Synthesis of Benzo[b]furans, in: 2015, pp. 261–376. Doi: 10.1016/bs.aihch.2015.08.003.

[49] M.M. Heravi, S. Khaghaninejad, N. Nazari, Bischler–Napieralski Reaction in the Syntheses of Isoquinolines∗, in: 2014, pp. 183–234. Doi: 10.1016/B978-0-12-

800171-4.00005-6.

[50] M.M. Heravi, T. Alishiri, Dimethyl Acetylenedicarboxylate as a Building Block in Heterocyclic Synthesis†, in: 2014, pp. 1–66. Doi: 10.1016/B978-0-12-800170-7.00001-8.

[51] S. Sadjadi, M.M. Heravi, M. Malmir, B. Masoumi, HPA decorated Halloysite Nanoclay: An efficient catalyst for the green synthesis of Spirooxindole derivatives, Appl. Organomet. Chem. 32 (3) (2018) e4113.

[52] S. Sadjadi, M.M. Heravi, M. Daraie, Heteropolyacid supported on amine-functionalized halloysite nano clay as an efficient catalyst for the synthesis of pyrazolopyranopyrimidines via four-component domino reaction, Res. Chem. Intermed. 43 (2017) 2201–2214, https://doi.org/10.1007/s11164-016-2756-8.

[53] M.M. Heravi, F. Mousavizadeh, N. Ghobadi, M. Tajbakhsh, A green and convenient protocol for the synthesis of novel pyrazolopyranopyrimidines via a one-pot, four-component reaction in water, Tetrahedron Lett. 55 (2014) 1226–1228, https://doi.org/10.1016/j.tetlet.2014.01.004.

[54] A. Tézé, M. Michelon, G. Hervé, Syntheses and structures of the tungstoborate anions, Inorg. Chem. 36 (1997) 505–509, https://doi.org/10.1021/ic961051t.

[55] A. Nisar, J. Zhuang, X. Wang, Cluster-based self-assembly: reversible formation of polyoxometalate nanocones and nanotubes, Chem. Mater. 21 (2009) 3745–3751, https://doi.org/10.1021/cm901305r.

[56] Y.-M. Nie, S.-H. Li, M.-Y. Lin, J. Yan, A micro-environment tuning approach for enhancing the catalytic capabilities of lanthanide containing polyoxometalate in the cyanosilylation of ketones, Chem. Commun. 56 (2020) 3809–3812, https://doi.org/10.1039/D0CC01216E.

[57] S. Arun, V.K. Singh, A. Naz, S.S. Narvi, P.K. Dutta, Journal of the Indian Chemical Society A comparative catalytic study using different metal ions by incorporating functionalized metallosalen into the lacunary position of Keggin polyoxometalate, J. Indian Chem. Soc. 98 (9) (2021) 100118.

[58] S.L. Giles, J.G. Lundin, R.B. Balow, P.E. Pehrsson, J.H. Wynne, Comparative roles of Zr^{4+} and Ni^{2+} Wells-Dawson hetero-metal substituted polyoxometalates on oxidation of chemical contaminants, Appl. Catal. A Gen. 542 (2017) 306–310, https://doi.org/10.1016/j.apcata.2017.06.002.

[59] S. Dastkhoon, Z. Tavakoli, S. Khodabakhshi, M. Baghernejad, M.K. Abbasabadi, Nanocatalytic one-pot, four-component synthesis of some new triheterocyclic compounds consisting of pyrazole, pyran, and pyrimidinone rings, New J. Chem. 39 (2015) 7268–7271, https://doi.org/10.1039/C5NJ01046B.

[60] S. Karami, M.G. Dekamin, E. Valiey, P. Shakib, DABA MNPs: a new and efficient magnetic bifunctional nanocatalyst for the green synthesis of biologically active pyrano[2,3- c]pyrazole and benzylpyrazolyl coumarin derivatives, New J. Chem. 44 (2020) 13952–13961, https://doi.org/10.1039/D0NJ02666B.

[61] M.A. Ghasemzadeh, B. Mirhosseini-Eshkevari, M.H. Abdollahi-Basir, MIL-53(Fe) metal-organic frameworks (MOFs) as an efficient and reusable catalyst for the one-pot four-component synthesis of pyrano[2,3-c]-pyrazoles, Appl. Organomet. Chem. 33 (1) (2019) e4679.

[62] L. Amiri-Zirtol, M.A. Amrollahi, Borax: an environmentally clean catalyst for the synthesize of pyrano[2,3-c]pyrazoles and xanthene-1,8-diones in H2O, Polycycl. Aromat. Compd. (2021) 1–12, https://doi.org/10.1080/10406638.2021.1954039.

[63] A.E. Method, R. Laroum, C. Boureghda, A. Benhadid, R. Boulcina, A. Debache, Study of the catalytic effect of sodium citrate on the four-component synthesis of pyrano [2, 3-c] pyrazole derivatives: an eco-friendly method, Indian J. Heterocycl. Chem. 27 (2018) 295–302.

[64] M. Zakeri, M.M. Nasef, T. Kargaran, A. Ahmad, E. Abouzari-Lotf, J. Asadi, Synthesis of pyrano[2,3-c]pyrazoles by ionic liquids under green and eco-safe conditions, Res. Chem. Intermed. 43 (2017) 717–728, https://doi.org/10.1007/s11164-016-2648-y.